Rabi oscillations in the optical pumping of a metastable neon beam with a cw dye laser

J. P. C. Kroon, H. A. J. Senhorst, H. C. W. Beijerinck, B. J. Verhaar, and N. F. Verster
Physics Department, Eindhoven University of Technology, 5600-MB Eindhoven, The Netherlands
(Received 6 June 1984; revised manuscript received 12 December 1984)

We report the measurement of Rabi oscillations in the optical pumping of a beam of metastable neon atoms in a three-level system with a cw dye laser. The laser beam is focused on the atomic beam, resulting in an interaction time with the laser beam of the order of the spontaneous lifetime of the induced transition. The Rabi oscillations are measured by a velocity-resolved analysis of the optically pumped metastable atoms. Adiabatic following is observed when the atoms cross the laser beam outside the waist, induced by the Doppler shifts due to the curvature of the wave fronts.

I. INTRODUCTION

The theory of Rabi oscillations describes the initial interaction of atoms with a coherent light source, predicting an oscillatory population of both the upper level and the lower level. The oscillatory behavior is basically caused by the coherence of the light. The oscillations are damped by spontaneous decay; therefore they can only be detected when the interaction time is of the order of the spontaneous lifetime of the transition used.

Rabi oscillations have been studied experimentally in different ways. The frequency-resolved fluorescence signal of a two-level system, using a high-resolution scannable Fabry-Perot interferometer, shows a three-peaked signal at a spacing equal to the Rabi nutation frequency.[1–3] Measurements are reported on the total fluorescence using a pulsed laser or using an electric field pulse for sweeping a group of atoms in and out of resonance by the Stark shift.[4,5] In our experimental configuration a laser beam is focused on a high-velocity beam [$v=(2-10)\times 10^3$ ms^{-1}], resulting in an interaction time of the same order as the spontaneous lifetime of the induced transition.

The same type of experimental arrangement for the measurement of Rabi oscillations on a vibrational infrared transition of SF_6 has been reported.[6] The longer lifetime of the transition allows the measurement of the oscillation with a thermal beam. The measurements reported here are the first measurements of this type in the visible spectral region.

The principle of adiabatic following is known from nuclear magnetic resonance measurements. It describes a two-level system being swept through resonance, resulting in the complete conversion of lower-level atoms to the upper level. The optical analog was measured on an infrared transition in NH_3.[7] In our experiment the adiabatic following can be observed when the atoms cross the laser beam outside the waist, where the curvature of the wave fronts causes a Doppler shift. For the case of a diverging laser beam the atoms initially observe a positive Doppler shift followed by a negative Doppler shift after passing the center line of the laser beam.

The experiment is done in a three-level system, i.e., the pumped metastable level, the excited level, which is populated by the laser interaction, and a third level which can be populated by spontaneous decay of the excited level. The existence of the third level causes the intensity of metastable atoms to decrease. We measure the attenuation of the metastable atoms, after passing the laser beam, as a function of their velocity, giving information on the pumping process.

II. THEORY

The relevant part of the energy diagram is given in Fig. 1. There are two metastable levels: the $1s_5$ and $1s_3$ levels with total angular momenta $J=2$ and 0, respectively. The laser is tuned to excite metastable atoms to one of the $2p$ levels. Spontaneous decay can occur to the pumped metastable level and to the other $1s$ levels. Spontaneous decay to the resonant $1s_2$ and $1s_4$ levels causes the intensity of the beam of metastable atoms to decrease.

A. Rabi oscillations without spontaneous decay

We briefly review the description of Rabi oscillations in a uniform laser field[8] and investigate the influence of the Gaussian envelope of the waist of a laser beam. The state $|\psi(t)\rangle$ of a two-level system is the superposition of the lower state $|a\rangle$ with energy $E_a=\hbar\omega_a$ and the upper state $|b\rangle$ with energy $E_b=\hbar\omega_b$, given by

$$|\psi(t)\rangle=c_a(t)\,|a\rangle e^{-i\omega_a t}+c_b(t)\,|b\rangle e^{-i\omega_b t}\,. \tag{1}$$

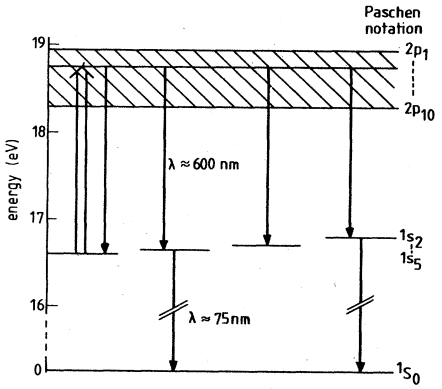

FIG. 1. Energy-level diagram of the Ne $1s$-$2p$ transitions, with Paschen notation for the excited states.

The state $|\psi(t)\rangle$ has to satisfy the time-dependent Schrödinger equation, with the Hamiltonian $H=H_0+H_1$ consisting of a contribution H_0 in absence of the laser field and a contribution H_1 due to the interaction of the atom with the field.

For the case of a linearly polarized laser beam (angular frequency ω, electric field amplitude $\mathbf{E}||\mathbf{z}'$) substitution of Eq. (1) in the time-dependent Schrödinger equation yields the usual differential equations

$$\frac{dc_a(t)}{dt}=\frac{i}{2}R_{ab}e^{-i\Delta\omega t}c_b(t)\ , \tag{2a}$$

$$\frac{dc_b(t)}{dt}=\frac{i}{2}R_{ba}e^{+i\Delta\omega t}c_a(t) \tag{2b}$$

in the rotating-wave approximation, with $|R_{ab}|=|-\langle a|\mu_{z'}|b\rangle E/\hbar|=|R_{ba}|=R$ the Rabi frequency, $\mu_{z'}$ the dipole moment along the z' axis, and $\Delta\omega=\omega_b-\omega_a-\omega$. The solution of Eqs. (2a) and (2b) is

$$|c_b(t)|^2=(R/\Omega)^2\sin^2(\Omega t/2)\ , \tag{3a}$$

$$\Omega=[R^2+(\Delta\omega)^2]^{1/2}\ . \tag{3b}$$

With the laser field on resonance ($\Delta\omega=0$) the upper-state population $|c_b(t)|^2$ has extrema for $Rt=n\pi$, with n integer and $n\geq 1$. Odd values correspond to maxima, even values to minima: The system has suffered a so-called $n\pi$ pulse. When the laser field is off resonance, i.e., $\Delta\omega\neq 0$, the oscillation depth decreases and the oscillation frequency increases.

In our experiment the atomic beam crosses a Gaussian laser beam in the waist. For this case Eqs. (2a) and (2b) are solved numerically for a time-dependent Rabi frequency $R(t)$, with the time t related to the position x in the laser beam according to

$$t=x/v\ . \tag{4}$$

A simple integration method has been used. Figure 2 shows the Rabi oscillations for atoms with a velocity $v=2\times 10^3\ \mathrm{m\,s^{-1}}$ as a function of x for a laser beam with

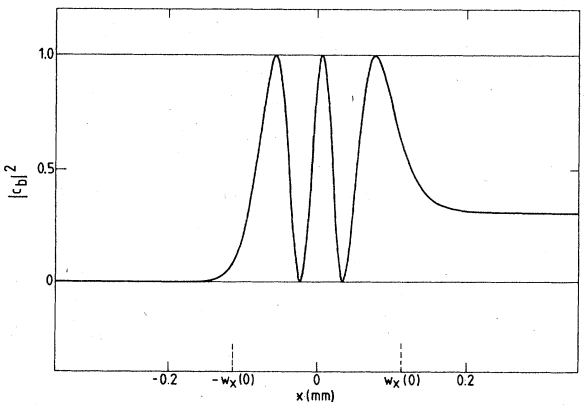

FIG. 2. Population of the upper level $|c_b(t)|^2$ as a function of the position x in the waist of the Gaussian laser beam, for a laser power $P=0.83$ mW. The waist radius $w_x(0)$ is also indicated.

dimensions according to Sec. III and total power $P=0.83$ mW. We observe that the oscillation frequency is larger at $x=0$ than for $x\neq 0$, as can be expected from the Gaussian profile of the electric field amplitude of the laser beam. Note that $x=w_x(0)$ corresponds to e^{-1} decrease of E and thus R.

B. Adiabatic following without spontaneous decay

In Sec. II A we have described Rabi oscillations for a uniform laser field, both for $\Delta\omega=0$ and for $\Delta\omega\neq 0$ but constant. When the angular frequency is time dependent, e.g., by sweeping the frequency of the laser field, the phase factor of the electromagnetic field is given by $\exp[i\int^t\omega(t')dt']$, resulting in a modified set of differential equations

$$\frac{dc_a(t)}{dt}=\frac{i}{2}R_{ab}c_b(t)\exp\left[-i\int_{-\infty}^{t}\Delta\omega(t')dt'\right]\ , \tag{5a}$$

$$\frac{dc_b(t)}{dt}=\frac{i}{2}R_{ba}c_a(t)\exp\left[+i\int_{-\infty}^{t}\Delta\omega(t')dt'\right] \tag{5b}$$

with the frequency difference $\Delta\omega(t)=\omega_b-\omega_a-\omega(t)$.

These equations are identical to those obtained in atom-atom scattering[9] for a system with two adiabatic potential curves with an avoided crossing, which has been initially investigated by Landau[10] and by Zener.[11] The energy difference of the diabatic curves for the atom-atom scattering as a function of the internuclear distance is replaced by the time-dependent energy difference $\hbar\Delta\omega(t)$. The energy $\hbar R$ is the equivalent of the coupling matrix element between the two adiabatic states. If we assume that

$$\Delta\omega(t)=\Delta\dot{\omega}(0)t\ , \tag{6a}$$

$$R(t)=R(0)\ , \tag{6b}$$

i.e., for the case of atom-atom scattering the diabatic curves are approximated by linear functions and the coupling matrix element does not depend on the internuclear distance, an analytical solution of Eqs. (5a) and (5b) is given by Zener.[11] For the boundary conditions $c_a(-\infty)=1$ and $c_b(-\infty)=0$, i.e., all atoms are in the lower level $|a\rangle$, the asymptotical behavior for $t\rightarrow\infty$ is given by

$$|c_a(\infty)|^2=\exp[-\pi R(0)^2/2\Delta\dot{\omega}(0)]\ , \tag{7a}$$

$$|c_b(\infty)|^2=1-|c_a(\infty)|^2\ . \tag{7b}$$

For $\Delta\dot{\omega}(0)\ll R(0)^2$ the system will follow the adiabatic curve and will end up in the upper level $|b\rangle$. This is usually called adiabatic following.

When the atomic beam in our experiment crosses the laser beam outside the waist, the curvature of the wave fronts results in a position-dependent Doppler shift. We find

$$\Delta\omega_D(x)=-\left[\frac{vx\omega}{c\rho_l}\right] \tag{8}$$

with ρ_l the radius of curvature of the wave front and x the position in the laser beam. Using Eq. (8) we find a

time-dependent frequency difference

$$\Delta\omega(t)=\omega_b-\omega_a-\omega-\Delta\omega_D(t)\ , \tag{9a}$$

$$\Delta\omega_D(t)=-\left[\frac{v^2\omega}{c\rho_l}\right]t \tag{9b}$$

with a constant rate of change proportional to v^2.

For a better qualitative understanding of the process of adiabatic following we can discuss this problem within the framework of a dressed atom. The diabatic energy curves for the initial and final states with $n+1$ and n photons, respectively, given by the product wave functions $|a\rangle|n+1\rangle$ and $|b\rangle|n\rangle$, are drawn in Fig. 3 for $n=0$. The finite slope of the $|a\rangle|1\rangle$ diabatic energy curve is due to the Doppler shift. However, the diabatic curves cannot cross and are connected by the dashed lines. If the rate of change of $\Delta\omega(t)$ is small in comparison to the square of the transition frequency $[R(0)]^2$ the system will follow the adiabatic curve.

In Fig. 4 the intensity contour of the laser beam and the atomic beam trajectory (2) are drawn. At a position $z_l=100$ mm from the waist and for a laser power $P=0.83$ mW Eqs. (5a) and (5b) have been solved numerically for the $\Delta m=0$ components of the $1s_5\rightarrow 2p_2$ transition in neon, using an average value of the Clebsch-Gordan coefficients (Sec. IV A). The population $|c_b(t)|^2$ as a function of the position x in the laser beam is given in Fig. 5, for velocities $v=2\times10^3$ and 10×10^3 m s^{-1} of the atom. By substituting the dimensions of the laser beam [Sec. III, Eq. (16)] we find $E(0)=1.93\times10^3$ V m^{-1}. Using Eqs. (2) and (17) to calculate the numerical value of $\langle a|\mu_{z'}|b\rangle$ we can determine the Rabi frequency on the axis of the laser beam $R(0)=1.02\times10^8$ s^{-1}. The radius of curvature is $\rho_l(z_l=100\text{ mm})=148$ mm. By inserting these numerical results in Eqs. (6), (7), and (9) we then find $|c_a(\infty)|^2=\exp(-56)$ and $\exp(-2.26)$ for $v=2\times10^3$ and 10×10^3 m s^{-1}, respectively. Comparison of these results with Fig. 5 is not very rewarding at first sight. We find $|c_a(\infty)|^2=4.7\times10^{-2}$ and 0 for $v=2\times10^3$ and 10×10^3 m s^{-1}, respectively.

We first discuss the results for $v=2\times10^3$ m s^{-1}. In Fig. 5 we observe a large number of oscillations superimposed on an adiabatic curve for $|c_b(t)|^2$. This indicates that we indeed are in the regime of adiabatic following. However, the Landau-Zener result is obtained by integration over a radiation field of infinite width and our numerical simulation only extends over the width of the laser beam, with a typical time scale $-\pi^{1/2}w_x(0)/2v\le t\le+\pi^{1/2}w_x(0)/2v$ [see Eq. (21)]. For $v=2\times10^3$ m s^{-1} this range is $-51\le t\le51$ ns. At time $t=51$ ns we find $\Delta\omega_D(51\text{ ns})=1.47\times10^7$ s^{-1}, which is small compared to $R(0)$. The difference between the diabatic curves at the onset of the laser beam is thus small in comparison with the effective separation at $t=0$ of the adiabatic curves in Fig. 3. In this respect it is hardly surprising that we observe large differences in comparison with the Landau-Zener formula. For $v=10\times10^3$ m s^{-1} we have a fully different situation. The curve in Fig. 5 is just a lucky example of a particle suffering a π pulse and should not be considered as due to adiabatic following. This is supported by the results for $v=20\times10^3$ m s^{-1}, which result in $|c_a(\infty)|^2=0.5$.

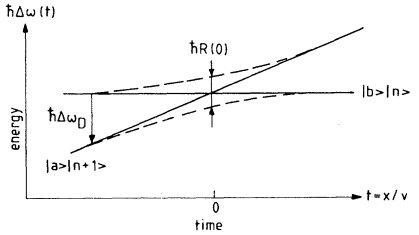

FIG. 3. Effective diabatic (solid line) and adiabatic (dashed line) potential-energy curves for the $|a\rangle|n+1\rangle$ and $|b\rangle|n\rangle$ states ($n=0$) of the dressed atom. The finite slope of the diabatic $|a\rangle|n+1\rangle$ curve is due to the position and thus time-dependent Doppler shift.

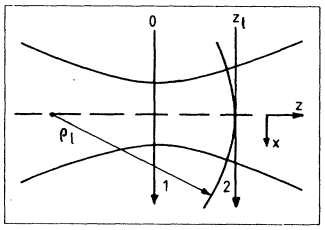

FIG. 4. The laser beam and two atomic trajectories, (1) resulting in Rabi oscillations, (2) resulting in adiabatic following. The e^{-2} intensity contour and the wave front at $z=z_l$ with radius $\rho_l(z)$ are also indicated.

C. Spontaneous emission

In Secs. II A and II B we have not taken into account the effect of spontaneous decay on the phenomena of Rabi oscillations and adiabatic following. Spontaneous decay of the upper level $|b\rangle$ to a third level can easily be incor-

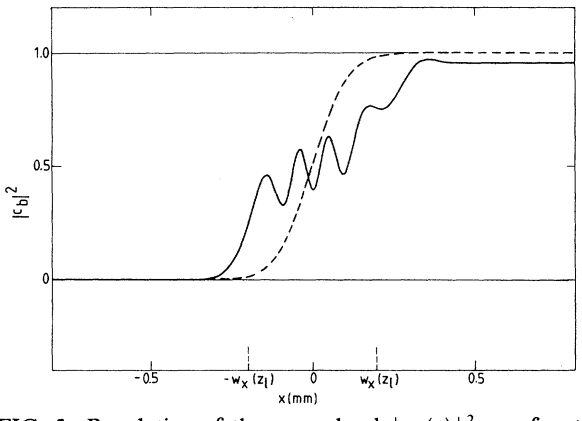

FIG. 5. Population of the upper level $|c_b(t)|^2$ as a function of the position x in the Gaussian laser beam. Laser power $P=0.83$ mW, $z_l=100$ mm, and waist length $L_x=70.6$ mm. The radius $w_x(z_l)=0.203$ mm is indicated in the horizontal scale. Velocity of atom $v=2000$ m s^{-1} (solid line); $v=10\times10^3$ m s^{-1} (dashed line).

porated in the semiclassical description given in Sec. II A by adding a semiempirical term $-(A_b/2)c_b(t)$ in Eq. (2b) with A_b the decay rate. Without the laser field the differential equation for $c_b(t)$ then becomes

$$\frac{dc_b(t)}{dt}=-(A_b/2)c_b(t)\ , \tag{10}$$

resulting in the usual rate equation for the population $|c_b(t)|^2$ of the upper level.

The analytical solution for the population of the upper level for the case of Rabi oscillations with only spontaneous decay to a third level, i.e., $A_b \gg A_{ba}$, is given by

$$|c_b(t)|^2=(R/\Omega)^2\sin^2(\Omega t/2)\exp[-(A_b/2)t]\ , \tag{11a}$$

$$\Omega=[R^2+(A_b/2)^2]^{1/2} \tag{11b}$$

for the case $\Delta\omega=0$. In comparison with Eq. (3) we see that the term $(A_b/2)^2$ has the same effect as $\Delta\omega^2$ for the case without spontaneous decay and causes an increase in oscillation frequency and a decrease in oscillation amplitude. Moreover, an extra damping with decay rate $A_b/2$ is added. The factor 2 in the decay rate can be understood qualitatively if we consider that the atom only spends half of its time in the upper level.

If we assume that $(A_b/2R)^2 \ll 1$ we can write the oscillation frequency as

$$\Omega \approx R\,[1+\tfrac{1}{2}(A_b/2R)^2]\ . \tag{12}$$

To determine the influence of the spontaneous decay on the oscillation frequency Ω we assume a damping with a factor $1/e$ for an interaction time $t=2\pi/\Omega\approx 2\pi/R$ resulting in the relation $(A_b/R)=1/\pi$. For these conditions we calculate $\Omega=1.013R$. We conclude that for those cases in which we observe Rabi oscillations, i.e., that they are not fully damped by spontaneous decay, the oscillation frequency is in good approximation given by the Rabi frequency R.

For adiabatic following, spontaneous decay to a third level can be included in Eqs. (5a) and (5b) in the same way as discussed previously. However, no analytical solution is available. For our experiment, where we detect the loss of atoms in the $|a\rangle$ level after the interaction, it is not important if the decay occurs during the interaction or at a later stage. We do not expect to observe any effect depending on the magnitude of the decay rate A_b.

We now discuss the limiting case $A_b=A_{ba}$, i.e., we only consider spontaneous decay from the upper level $|b\rangle$ to the lower level $|a\rangle$. Spontaneous emission of a photon by the upper state of the atom (with a wave function with a well-defined initial phase) will result in a product wave function of the atomic lower state and the photon state, with the same well-defined phase. Subtracting the information on the emitted photon, in which we are not interested, will leave us with the lower-level wave function with a random phase. This process is illustrated in Fig. 6, which gives the amplitudes $c_b(t)$ and $c_a(t)$ in the complex plane. Subsequent spontaneous decay decreases the amplitude $c_b(t)$ according to Eq. (10) with amounts $\Delta_i \sim c_b(t)\Delta t$. The amplitude $c_a(t)$, however, is modified by adding equal contributions $\Delta c_a(t)=|\Delta_i|\exp(i\phi)$ with a random phase ϕ. A time average then results in

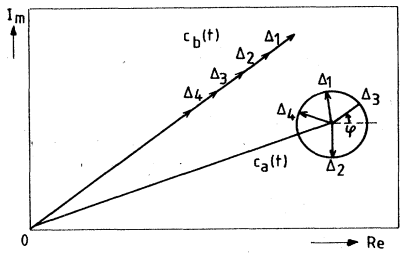

FIG. 6. Decrease of the complex amplitude $c_b(t)$ of the upper level with $\Delta_i \sim c_b(t)\Delta t$ due to spontaneous decay results in an increase of the amplitude $c_a(t)$ of the lower level with $\Delta c_a(t)=|\Delta_i|\exp(i\phi)$ with a random phase ϕ.

$$\frac{dc_a(t)}{dt}=0\ , \tag{13a}$$

$$\frac{d|c_a(t)|^2}{dt}=A_{ba}|c_b(t)|^2\ , \tag{13b}$$

where the latter describes [together with Eq. (10)] the conservation of particles.

These equations directly show that for this case spontaneous emission cannot be included in the semiclassical description by adding an extra semiempirical term in the differential equations for the amplitudes $c_a(t)$ and $c_b(t)$ [Eqs. (2) and (5)]. Although the quantum field theory provides a rigorous solution of spontaneous decay,[12] we propose a more straightforward description in terms of the density matrix operator $\rho(t)$ because we are only interested in the atomic state. By using the relation

$$\frac{d[c_a^*(t)c_b(t)]}{dt}=c_a^*(t)\frac{dc_b(t)}{dt}+\frac{dc_a^*(t)}{dt}c_b(t)$$
$$=-\frac{A_{ba}}{2}c_a^*(t)c_b(t) \tag{14}$$

the equation for the time evolution of $\rho(t)$ becomes

$$\frac{d\rho(t)}{dt}=\frac{i}{\hbar}[\rho(t),H_1]$$
$$+A_{ba}\begin{pmatrix}\rho_{bb}(t) & -\frac{1}{2}\rho_{ab}(t)\\ -\frac{1}{2}\rho_{ab}(t) & -\rho_{bb}(t)\end{pmatrix} \tag{15}$$

with the first term on the right-hand side describing the interaction with the electromagnetic field and the second term due to spontaneous decay.

In our experiment we detect the loss of atoms in the metastable $|a\rangle$ level after the interaction with the laser beam. This loss is caused by decay of the upper $|b\rangle$ level to the resonant levels. The transitions used are therefore characterized by $A_b \gg A_{ba}$ and the results of Eq. (11) are valid in good approximation. For application to an arbitrary system, where A_{ba} may play an important role, Eq. (15) is a good starting point when the effect of decay to a third level with rate A_b-A_{ba} is added. For the resonant case $\Delta\omega=0$ this will result in damped Rabi oscillations due to the loss of coherence on a time scale of the lifetime A_{ba}^{-1}.[13]

III. EXPERIMENTAL CONDITIONS

The experimental setup has been described in detail elsewhere.[14] Here we give the main features (Fig. 7). The atomic beam is produced by a hollow cathode arc which is an intense source[15] for metastable atoms with translational energies in the range 1—10 eV. A single-mode, frequency-stabilized (0.5 MHz rms) cw dye laser was used which was locked to the absolute transition frequency using an auxiliary atomic beam setup.[16]

The laser beam and the atomic beam cross at right angles. A cylindrical lens with focal length $F=200$ mm is used to decrease the waist size of the laser beam along the atomic beam (x axis, see Fig. 7), resulting in a waist radius $w_x(0)=0.115$ mm (e^{-2} intensity contour) with waist position $z=0$ at the crossing point. The waist of the laser beam perpendicular to the atomic beam (y direction, see Fig. 7) is positioned before the crossing point at $z=-194$ mm, with a waist radius w_y ($z=194$ mm)$=0.314$ mm. At $z=0$ the radius in the y direction is thus $w_y(0)=0.335$ mm. With a collimator of 0.3-mm diameter in the atomic beam, careful alignment in the y direction then results in an electric field which is constant within 4% over the height of the atomic beam. This is done with a plane-parallel plate which enables a vertical scan of 0.5 mm with a high reproducibility. By moving the lens along the z direction the waist in the x direction can be centered on the atomic beam axis. For the waist in the x direction the divergence is $\alpha_x=1.63$ mrad (half angle) and the waist length is $L_x=70.6$ mm, as follows directly from the wavelength ($\lambda=588.1$ nm for the $1s_5\rightarrow 2p_2$ transition) and the waist radius $w_x(0)$.

The relation between the amplitude $E(0)$ of the electric field on the center line and the total power P of the laser beam is given by

$$E(0)=\left[\frac{\pi}{4}\epsilon_0 c w_x(z) w_y(z)\right]^{-1/2} P^{1/2}$$

$$=G(z)P^{1/2} \tag{16}$$

with $G(z)$ determined by the geometry of the laser beam and ϵ_0 the permittivity of vacuum. By substituting the beam dimensions at $z=0$ we find $G(0)=3.53\times 10^3$ $\mathrm{V\,m^{-1}\,mW^{-1/2}}$. In our experiment the total power P is measured with a commercial laser power meter[17] without any extra calibration in our laboratory.

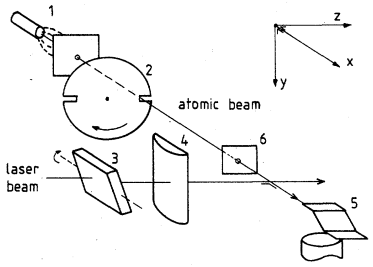

FIG. 7. Experimental setup. (1) Hollow cathode arc, (2) chopper, (3) plane-parallel plate, (4) cylindrical lens, (5) detector of metastable atoms, (6) collimator 0.3-mm diameter.

The experiments have been performed with a linearly polarized laser beam, resulting in a matrix element [Eq. (2)]

$$\langle a\,|\mu_{z'}|\,b\rangle=\frac{(J_a m_a 10\,|\,J_b m_b)}{(2J_b+1)^{1/2}} e\langle J_a||r||J_b\rangle \tag{17}$$

with $(J_a m_a 10\,|\,J_b m_b)$ the Clebsch-Gordan coefficient and $\langle J_a||r||J_b\rangle$ the reduced matrix element, with the selection rule $\Delta m=m_a-m_b=0$ for transitions between the different magnetic substates. For a $J_a=0$ to $J_b=1$ transition we only excite the $|00\rangle$ to $|10\rangle$ component, which is possible by choosing the $1s_3$ ($J_a=0$) metastable state as a lower level. However, we have used the $1s_5$ ($J_a=2$) metastable state as a lower level, which according to the statistical weight is most abundant. For an upper level with $J_b=1$ or 2 we then simultaneously excite three or four $\Delta m=0$ components, respectively. The different Clebsch-Gordan coefficients for these $\Delta m=0$ components will result in Rabi oscillations with different frequencies R. The best choice is $J_b=1$, where the numerical values are $(2010|10)=(\frac{4}{10})^{1/2}$ and $(2110|11)=(\frac{3}{10})^{1/2}$. The first three oscillations are thus almost in phase.

Our final choice as upper level is the $2p_2$ ($J_b=1$) level with decay rates[18] $A_{ba}=1.28\times 10^7\ \mathrm{s^{-1}}$ and $A_{bc}=4.73\times 10^7\ \mathrm{s^{-1}}$. The latter is the sum of the decay rate $A_{br}=3.13\times 10^7\ \mathrm{s^{-1}}$ to the $1s_2$ and $1s_4$ resonant levels (with a uv cascade to the ground state) and the decay rate $A_{bm}=1.60\times 10^7\ \mathrm{s^{-1}}$ to the $1s_3$ metastable level. The wavelength of the $1s_5\rightarrow 2p_2$ transition is $\lambda=588.1$ nm. From the value of A_{ba} we can directly derive the numerical value[19] $e\langle J_b||r||J_a\rangle=1.66\times 10^{-29}$ C m or use the line strengths listed.[18]

The $1s_5\rightarrow 2p_2$ transition thus combines a large attenuation of the beam of metastable atoms by decay of the $2p_2$ level to the resonant levels with a small difference in Rabi-oscillation frequencies for the different $\Delta m=0$ components.

The beam of metastable atoms is analyzed using time-of-flight techniques. The metastable atoms are detected by secondary emission on a stainless-steel surface and subsequent multiplication with a CuBe multiplier.

IV. RESULTS

A. The Rabi oscillations as a function of the laser power

After crossing the laser beam, the Rabi oscillations will leave the atoms in the upper level (a $n\pi$ pulse with n odd), in the lower level (n even), or in an intermediate situation with atoms in both the upper and lower levels, depending on the electric field of the applied laser beam and the interaction time of the atoms with the field, i.e., the velocity of the atoms. Atoms in the upper level will decay spontaneously to both the metastable levels and the resonant levels. The atoms decaying to the resonant levels and subsequently to the ground level give rise to the attenuation of the beam of metastable atoms. The group of atoms in the lower level, after crossing the laser beam, will remain there.

We measure two time-of-flight spectra: one with the laser switched off and one with the laser switched on. We define the population ratio $\epsilon(v)$ as the intensity $I_{on}(v)$ with laser on divided by the intensity $I_{off}(v)$ with the laser off, as given by

$$\epsilon(v)=\frac{I_{on}(v)}{I_{off}(v)} . \tag{18}$$

Figure 8 shows $\epsilon(v)$ as a function of the velocity of the atoms for a laser power $P=6.1$ mW. One clearly sees the minimum for $1/v=0.07\times10^{-3}$ $(\mathrm{m\,s^{-1}})^{-1}$ indicating that the upper level of the atom was populated after crossing the laser beam. The atoms with this velocity have suffered a π pulse and the minimum will be denoted the $\epsilon(v_\pi)$ minimum. The maximum for $1/v=0.13\times10^{-3}$ $(\mathrm{m\,s^{-1}})^{-1}$ is from atoms in the lower level after leaving the laser beam. These atoms have suffered a 2π pulse and the maximum will be denoted the $\epsilon(v_{2\pi})$ maximum. Due to the spontaneous decay while passing the laser beam we find $\epsilon(v_{2\pi})<1$.

For comparison with our experiments we now derive an expression for the velocity $v_{n\pi}$ which is necessary for a $n\pi$ pulse while crossing the laser beam. Because the laser beam has a Gaussian profile, the Rabi frequency $R(t)$ is the time dependent and the simple relation $Rt=n\pi$ of Sec. II A cannot be used any longer. In this case a $n\pi$ pulse is determined by the relation

$$\Phi=\int_{-\infty}^{+\infty} R(t)dt=n\pi \tag{19}$$

with Φ the phase of the Rabi oscillation after the interaction with the laser beam. By substituting the numerical value of the reduced matrix element (Sec. III) and the average value $\frac{1}{3}[2(\frac{3}{10})^{1/2}+(\frac{4}{10})^{1/2}]=0.58$ of the Clebsch-Gordan coefficient of the three components into Eqs. (2) and (17) we find the time-dependent Rabi-oscillation frequency $R(t)$ for an atom traveling through the laser beam, as given by

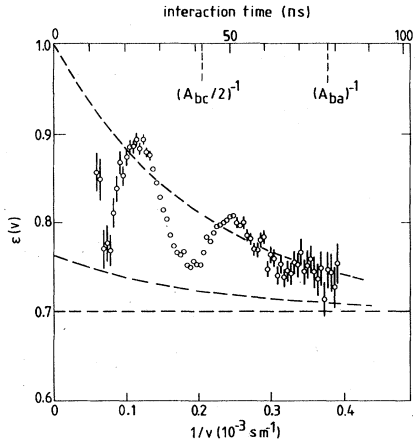

FIG. 8. Experimental results for the population ratio $\epsilon(v)$ as a function of the inverse velocity of the atoms, revealing the effect of Rabi oscillations. The upper scale gives the interaction time with the laser according to $t=\pi^{1/2}w_x(0)/v$. The dashed lines are predictions for the $n\pi$ minima and maxima, respectively, according to Eqs. (24) and (25).

$$R(t)=(5.26\times10^{4}\ \mathrm{m\,V^{-1}\,s^{-1}})E(t) \tag{20}$$

with $E(t)$ the position [=time, see Eq. (4)]-dependent electric field amplitude of the laser beam. By inserting $E(t)=E(0)\exp\{-[vt/w_x(0)]^2\}$, with $E(0)$ the amplitude on the center line, we find the relation

$$\Phi=(5.26\times10^{4}\ \mathrm{m\,V^{-1}\,s^{-1}})\frac{E(0)\pi^{1/2}w_x(0)}{v} . \tag{21}$$

This expression is equivalent to the case of a homogeneous electric field with width $\pi^{1/2}w_x(0)$. If we look at Fig. 2 this seems a realistic measure of the effective width of the interaction region. By combining Eq. (19) with Eqs. (16) and (21) we can now write the velocity $v_{n\pi}$ as a function of the power P of the laser, resulting in

$$v_{n\pi}=(5.26\times10^{4}\ \mathrm{V\,m^{-1}\,s^{-1}})\frac{G(0)w_x(0)}{\pi^{1/2}}\frac{P^{1/2}}{n} \tag{22a}$$

$$=\alpha_{theor}\left[\frac{P^{1/2}}{n}\right] . \tag{22b}$$

Figure 9 gives the velocity $v_{n\pi}$ for $n=1$, 2, and 3 as a function of $P^{1/2}$ for a series of measurements. The data were analyzed with a single parameter α_{expt}, which is the experimental counterpart of α_{theor} in Eq. (22b). We find

$$\alpha_{expt}=0.65\times10^{4}\ \mathrm{m\,s^{-1}\,mW^{-1/2}} , \tag{23a}$$

$$\alpha_{theor}=1.20\times10^{4}\ \mathrm{m\,s^{-1}\,mW^{-1/2}} , \tag{23b}$$

where the theoretical value has been calculated by inserting the laser beam dimensions of Sec. III into Eq. (22a). In our opinion the difference is due to the experimental measurement of the power P. All other parameters are well known or can be calculated accurately from other input parameters. Still, it is rather surprising that the power meter indicates powers which are a factor 3.4 larger than the actual values.

When the laser frequency is stabilized on the absolute transition frequency (which is the case in our configuration) the atomic beam must be exactly perpendicular to the laser beam in order to observe the on-resonance Rabi oscillations. A misalignment of 1 mrad will cause atoms with a velocity $v=8000$ m/s to see the laser frequency

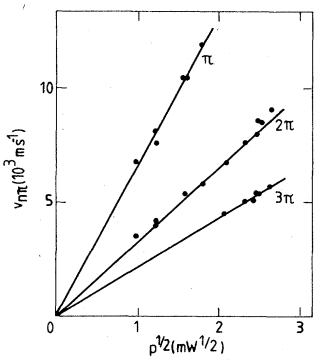

FIG. 9. Experimental results for the velocity $v_{n\pi}$ ($n=1$, 2, and 3) as a function of $P^{1/2}$, with P the power of the laser beam, with the straight line curve fit $v_{n\pi}=\alpha_{expt}(P^{1/2}/n)$ [Eq. (23a)].

Doppler shifted by $\Delta\omega_D = 8.4\times10^7$ rad/s. A laser power $P=1$ mW results in an electric field amplitude on the laser beam axis $E_0 = 3.5\times10^3$ V/m for the laser beam dimensions used [Eq. (16)]. According to Eqs. (20) and (3) a misalignment of 1 mrad therefore decreases the amplitude of the Rabi oscillations by a factor 0.63. Moreover, the $1/n$ dependency of the straight lines of Fig. 9 will be violated. A very careful alignment of the beams is essential to obtain these results. Using a computer-driven mirror with both a rotational and a translational degree of freedom we can obtain a perpendicular alignment with a reproducibility better than 0.2 mrad.[20]

B. The $\epsilon(v_\pi)$ minimum and the $\epsilon(v_{2\pi})$ maximum

To describe our experimental data of the population ratio $\epsilon(v_{n\pi})$ we have to discuss the beam composition in detail. First, we have to take into account the isotope composition. We assume natural abundance according to ^{20}Ne:^{22}Ne=0.909:0.091. Second, we assume a distribution according to the statistical weight $^{20}\mathrm{Ne}(1s_5)$:$^{20}\mathrm{Ne}(1s_3)$ =5:1. This is supported by previous measurements.[14] If we consider that only three magnetic substates $m_a=-1$, 0, and $+1$ are optically pumped in the $1s_5\rightarrow2p_2$ transition, the resulting fraction of atoms in the $|a\rangle$ level is 0.454, i.e., a lower limit for the population ratio is $\epsilon(v)\geq0.546$.

For the fraction of the atoms in the $|a\rangle$ level we have to determine which part ends up in the metastable levels after the interaction with the laser beam, i.e., is detected by the atomic beam detector. In first approximation we neglect the damping of the Rabi oscillations due to the decay rate A_{ba} (Sec. II C). After a π, 3π, 5π, etc., pulse a fraction $[1-\exp(-A_{bc}t/2)]$ of the population of the $|a\rangle$ level has decayed to the $|c\rangle$ levels by spontaneous decay during the interaction [Eq. (11a)]. The branching ratios of this decay to the metastable $1s_3$ level and the resonant $1s_2$ and $1s_4$ levels are A_{bm}/A_{bc} and A_{br}/A_{bc}, respectively (Sec. III). The remaining fraction $\exp(-A_{bc}t/2)$ leaves the laser beam in the $|b\rangle$ level. By taking into account the branching ratios of the decay of the $|b\rangle$ level to the metastable $1s_5$ and $1s_3$ levels and the resonant $1s_2$ and $1s_4$ levels, given by $(A_{ba}+A_{bm})/A_b$ and A_{br}/A_b, respectively, we find the following expression for the beam population ratio:

$$\epsilon(v_{n\pi})=0.546+0.454\left[\frac{A_{bm}}{A_{bc}}+\left[\frac{A_{ba}+A_{bm}}{A_b}-\frac{A_{bm}}{A_{bc}}\right]\exp(-A_{bc}t/2)\right]$$
$$=0.699+0.063\exp\left[-\frac{4.82\times10^3\ \mathrm{m\,s^{-1}}}{v_{n\pi}}\right] \qquad (24)$$

(n odd), where the latter has been obtained by substituting the numerical values of the decay rates for the $2p_2$ level (Sec. III). For an estimate of the interaction time, we have used $t=\pi^{1/2}w_x(0)/v_{n\pi}$, i.e., we have assumed an effective width $\pi^{1/2}w_x(0)$ of the laser beam.

For a 2π, 4π, 6π, etc., pulse the only difference from the previous case is that the remaining fraction $\exp(-A_{bc}t/2)$ of the atoms is in the $|a\rangle$ level and are all detected. We find

$$\epsilon(v_{n\pi})=0.546+0.454\left[\frac{A_{bm}}{A_{bc}}+\frac{A_{br}}{A_{bc}}\exp(-A_{bc}t/2)\right]$$
$$=0.699+0.301\exp\left[-\frac{4.82\times10^3\ \mathrm{m\,s^{-1}}}{v_{n\pi}}\right] \qquad (25)$$

(n even), using the same input as Eq. (24). The curves of Eqs. (24) and (25) are plotted in Fig. 8. We observe a fair agreement. The deviations are due to the damping of the amplitude of the Rabi oscillations as predicted by Eq. (11), both due to the upper-level decay rate A_{ba} and the difference in Rabi frequencies of the $m_a=\pm1$ and 0 magnetic substates. A numerical simulation shows that the latter amounts to a decrease in amplitude of 5% and 10% for a 2π and 3π pulse, respectively. At long interaction times $t\simeq(A_{ba})^{-1}$ the first effect will dominate; at short interaction times (i.e., high laser powers) the latter effect will be dominant.

In Fig. 10 we have plotted the $\epsilon(v_\pi)$ minima and the $\epsilon(v_{2\pi})$ maxima as a function of the inverse velocity $1/v$ of the atoms for different laser powers P. The experimental values for the $\epsilon(v_{2\pi})$ maxima have been analyzed with a model function similar to Eqs. (24) and (25), using a least-squares method to determine the three parameters. The result is

$$\epsilon(v_{2\pi}(P))=0.767+0.221\exp\left[-\frac{4.73\times10^3\ \mathrm{m\,s^{-1}}}{v_{2\pi}(P)}\right]. \qquad (26)$$

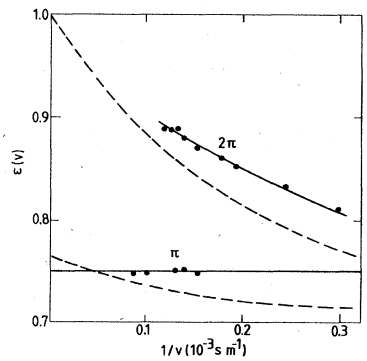

FIG. 10. Experimental values of the $\epsilon(v_\pi)$ minimum and the $\epsilon(v_{2\pi})$ maximum as a function of the inverse velocity of the atoms, for different values of the total power P of the laser beam. The solid lines indicate the curve fit according to Eqs. (26) and (27); the dashed lines are the results of a simple model according to Eqs. (24) and (25).

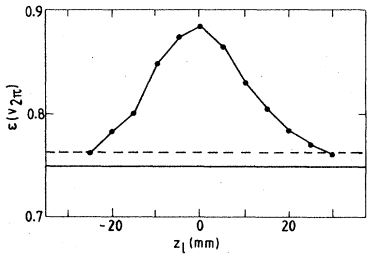

FIG. 11. Experimental results for the $\epsilon(v_{2\pi})$ maximum as a function of the distance z_l between the atomic beam and the waist of the laser beam in the x direction. Solid line, curve fit of $\epsilon(v_\pi)$ minimum [Eq. (27)]; dashed line, prediction for $\epsilon(v)$ at conditions of adiabatic following [Eq. (28)].

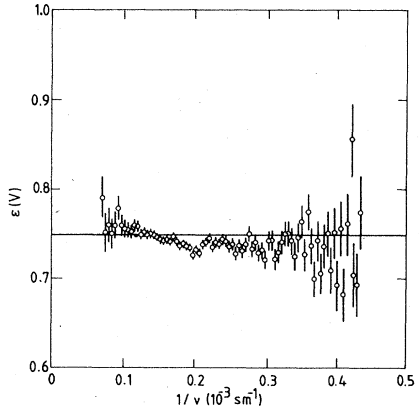

FIG. 12. Experimental results for the population ratio $\epsilon(v)$ as a function of the inverse velocity of the atoms at $z_l=25$ mm and $P=4.6$ mW, revealing the effect of the process of adiabatic following. Solid line, experimental result for $\epsilon(v_\pi)$ [Eq. (27)].

In comparison with the theoretical prediction of Eq. (25) we observe an excellent agreement for the effective decay rate in the exponent. Due to a correlation of the preexponential factor with the constant term in the model function, the agreement for these parameters is less satisfactory. The curve fit of Eq. (26) is plotted in Fig. 10, together with the prediction of Eq. (25).

The $\epsilon(v_\pi)$ minima have only been analyzed by calculating their average value because it is impossible to determine the three parameters of the model function separately, resulting in

$$\epsilon(v_\pi)=0.75\ . \tag{27}$$

The deviations of this value from the predictions of Eq. (24) have already been discussed. Equation (27) is also plotted in Fig. 10.

C. Adiabatic following

The Rabi oscillations in the population ratio $\epsilon(v)$ disappear when the atomic beam crosses the laser beam outside the waist. Figure 11 shows the $\epsilon(v_{2\pi})$ as a function of the distance z_l between the atomic beam and the waist in the x direction (Fig. 3). The experimental value of the velocity is $v_{2\pi}=7\times10^3$ m s^{-1} at position $z_l=0$; the measured power of the laser beam is $P=4.6$ mW. At a distance $z_l=5$ mm the $\epsilon(v_{2\pi})$ maximum has already decreased drastically. At $z_l=25$ mm the $\epsilon(v_{2\pi})$ maximum has almost disappeared, if we compare it to the average value $\epsilon(v_\pi)=0.75$ from Fig. 10. This cannot be explained by an increase in spontaneous decay due to the increase in interaction time, which is caused by the larger radius $w_x(z_l)$ of the laser beam. This increase is less than 6% for $z_l\leq25$ mm, as follows from the waist length L_x and the usual relation for the radius of a Gaussian laser beam,[21] and would result in only a very small effect (Fig. 10).

In view of our discussion in Sec. II B the only correct interpretation is found in the model of adiabatic following. At $z_l=25$ mm we have a radius of curvature equal to $\rho_l=224$ mm, and we are close to the conditions of the numerical simulation discussed in Sec. II B. By assuming that $|c_b(t)|^2=1$ after the interaction with the laser beam, the population ratio $\epsilon(v)$ directly follows from the branching ratio $(A_{bm}+A_{ba})/A_b$ for spontaneous decay to the metastable $1s_3$ and $1s_5$ levels, resulting in

$$\epsilon(v)=0.546+0.454\left[\frac{A_{bm}+A_{ba}}{A_b}\right]$$
$$=0.764\ . \tag{28}$$

In Fig. 12 we show the population ratio $\epsilon(v)$ at $z=25$ mm and $P=4.6$ mW, together with the experimental result of Eq. (27) for the value of the $\epsilon(v_\pi)$ minimum. We observe a slight increase of $\epsilon(v)$ for increasing velocities v, i.e., a decreasing interaction time. However, the nearly constant experimental result for $\epsilon(v)$ is still very different from Fig. 8. We conclude that the measurements support our analysis in Sec. II B and reveal the features of adiabatic following in a very convincing way.

V. DISCUSSION

Using the high-velocity atomic beam of a hollow cathode arc and a laser beam focused to a small waist diameter, all features of the interaction of a coherent laser beam and an atomic beam can be measured. Rabi oscillations and adiabatic following have been observed. The experimental results are in good agreement with theory. These measurements are the first of this type in the visible spectral region; moreover, a very good accuracy is obtained. In more commonly used optical-pumping schemes, for instance with a thermal atomic beam and a nonfocused laser beam, it is impossible to observe these features because they are completely damped by spontaneous decay.

The method of adiabatic following shows large promise for applications in beam experiments with atoms in short-lived excited states. In these experiments the velocity-dependent Rabi oscillations are highly undesirable, because they can easily introduce an artificial velocity dependency in the cross sections for the collision processes investigated.

Note added in proof. The power meter has been calibrated and shows the correct reading within 10%. Therefore, the difference between the experimental and theoretical values of Eqs. (23a) and (23b) is not understood at this moment. Here we give the relation used to calculate the reduced matrix element

$$A_{ba}=\frac{1}{2J_b+1}\frac{\omega_0^3}{3\pi\epsilon_0\hbar c^3}e^2|\langle J_b||r||J_a\rangle|^2 .$$

Inserting Eq. (29) into Eqs. (17) and (2) then results in the Rabi frequency R as a function of the electric field E according to Eq. (20).

[1]W. Hartig, W. Rasmussen, R. Schieder, and H. Walther, Z. Phys. A **278**, 205 (1976).

[2]R. E. Grove, F. Y. Wu, and S. Ezekiel, Phys. Rev. A **15**, 227 (1977).

[3]F. Schuda, C. R. Strout, Jr., and M. Herscher, J. Phys. B **7**, L198 (1974).

[4]H. M. Gibbs, Phys. Rev. A **8**, 446 (1973).

[5]W. R. MacGillivray and M. C. Standage, Opt. Commun. **36**, 189 (1981).

[6]S. Avrillier *et al.*, Opt. Commun. **39**, 311 (1981).

[7]M. M. T. Loy, Phys. Rev. Lett. **32**, 814 (1974).

[8]See, for example, M. Sargent III, M. O. Scully, and W. E. Lamb, *Laser Physics* (Addison-Wesley, Reading, Mass., 1974).

[9]D. R. Bates, Proc. R. Soc. London, Ser. A **257**, 22 (1960).

[10]L. Landau, Z. Phys. Sowjet. **2**, 4 (1932).

[11]C. Zener, Proc. R. Soc. London, Ser. A **137**, 696 (1932).

[12]B. R. Mollow and M. M. Miller, Ann. Phys. (N.Y.) **52**, 464 (1969).

[13]See, for example, R. Loudon, *The Quantum Theory of Light* (Clarendon, Oxford, 1983).

[14]J. P. C. Kroon, H. C. W. Beijerinck, B. J. Verhaar, and N. F. Verster, Chem. Phys. **90**, 195 (1984); J. P. C. Kroon, H. C. W. Beijerinck, and N. F. Verster, J. Chem. Phys. **74**, 6528 (1981).

[15]P. G. A. Theuws, H. C. W. Beijerinck, N. F. Verster, and D. C. Schram, J. Phys. E **15**, 573 (1982).

[16]M. J. Verheijen, H. C. W. Beijerinck, and N. F. Verster, J. Phys. E **15**, 1198 (1982).

[17]Newport Research Corporation Model 820 laser power meter.

[18]W. L. Wiese, M. W. Smith, and B. M. Glennon, *Atomic Transition Probabilities,* Natl. Bur. Stand. Ref. Data Ser., Natl. Bur. Stand. (U.S.) Circ. No. 4 (U.S. GPO, Washington, D.C., 1966), Vol. I.

[19]See, for example, I. I. Sobelman, *Atomic Spectra and Radiative Transitions* (Springer, New York, 1979).

[20]M. J. Verheijen, H. C. W. Beijerinck, and N. F. Verster, Rev. Sci. Instrum. (to be published).

[21]See, for example, A. E. Siegman, *An Introduction to Lasers and Masers* (McGraw-Hill, New York, 1971).